### International Journal of MATERIALS RESEARCH

Zeitschrift für METALLKUNDE

## Original Contributions

M. C. Somani et. al.: Static recrystallization characteristics and kinetics of high-silicon steels for direct quenching

Mahesh C. Somani<sup>a</sup>, David A. Porter<sup>a</sup>, L. Pentti Karjalainen<sup>a</sup>, Pekka K. Kantanen<sup>a</sup>, Jukka I. Kömi<sup>a</sup>, Devesh K. Misra<sup>b</sup>

<sup>a</sup>University of Oulu, Faculty of Technology, Centre for Advanced Steels Research, Oulu, Finland

# Static recrystallization characteristics and kinetics of high-silicon steels for direct quenching and partitioning

In the direct quenching and partitioning (DQ&P) process, tough ultra-high-strength steel is made by combining thermomechanical processing with quenching and partitioning to obtain martensite toughened by thin films of retained austenite. The hot rolling stage with deformation and recrystallization between the rolling passes affects the state of the austenite before quenching and partitioning. This paper describes the static recrystallization kinetics of two steels with compositions suited to DQ&P processing, viz. (in wt.%) 0.3C-1Si-2Mn-1Cr and 0.25C-1.5Si-3Mn. The stress relaxation technique on a Gleeble thermomechanical simulator provided recrystallization times over a wide range of temperature, strain, strain rate and initial grain size. The higher levels of Si and Mn made the recrystallization kinetics less sensitive to strain, strain rate and temperature. The equations derived to describe the recrystallization kinetics can be used in the design of the rough rolling part of thermomechanical processing.

**Keywords:** Recrystallization; Flow stress; Stress relaxation; Austenite; Direct quenching and partitioning

### 1. Introduction

In recent years, extensive efforts have been directed to the development of ultra-high-strength steels with excellent combinations of mechanical properties such as high strength, good ductility, low-temperature toughness and reasonable formability. This, however, requires optimal design of new, inexpensive compositions besides developing innovative thermomechanical processing (TMCP) routes to meet the new challenges. Conventionally, quenching and tempering is used to obtain high-strength structural steels with good impact toughness. The ductility of these steels in terms of their elongation or reduction of area to fracture in uniaxial tensile testing is generally acceptable, but their uniform elongation, i.e. work hardening capacity is relatively low. This deficiency is an important factor limiting the wider application of such steels because strain localization during fabrication or as a result of overloading in the final application can be detrimental to the integrity of the structure.

A novel concept of quenching and partitioning (Q&P) has been proposed as a potential processing route for improving the balance of elongation to fracture and tensile strength for advanced high-strength steels [1–3]. In the Q&P processing, the steel is austenitized, quenched to a temperature between the martensite start ( $M_s$ ) and finish ( $M_f$ ) temperatures and held at a suitable temperature for a suitable time to allow the partitioning of carbon from martensite to austenite, which can thereby be partly or fully stabilized down to room temperature. Unlike in the case of tempering, the formation of iron carbides and the decomposition of austenite are intentionally suppressed by the use of

<sup>&</sup>lt;sup>b</sup>University of Texas at El Paso, Dept. of Metallurgical, Materials and Biomedical Engineering, El Paso, TX, USA

Si, Al or P alloying [1-6]. A martensitic matrix has the potential to provide the required high strength, while a small fraction of finely divided austenite stabilized between the martensitic laths provides the desired uniform elongation and improved work hardening via transformation induced plasticity (TRIP). Based on the principles of the Q&P process, a novel processing route comprising thermomechanical rolling followed by direct quenching and partitioning (TMR-DQP) has recently been developed with the aim of achieving yield strength ≥1 100 MPa combined with good ductility and impact toughness [7-11]. This, however, requires that the thermomechanically controlled rolling is optimized with respect to both recrystallization above the recrystallization limit temperature (RLT) as well as controlled rolling in the narrow range between the recrystallization stop temperature (RST) and  $A_{r3}$  temperatures. There are only a few papers dealing with the DQP process, though reporting promising strength and ductility combinations [12, 13].

In the course of developing the TMR-DQP process, a two-pronged approach was adopted in order to first optimize the TMCP parameters with the aid of physical and laboratory rolling simulation studies and then to design appropriate direct quenching and partitioning schedules to achieve the desired properties [7-11]. The chosen approach was to design suitable chemical compositions based on high silicon contents and find appropriate TMCP processing conditions with the aid of physical simulation on a Gleeble simulator. In addition, dilatation measurements and electron microscopy studies were combined with published information to understand the possible microstructural mechanisms operating during Q&P processes. The specific aim was to develop a steel with a yield strength of the order of  $\sim 1\,100\,\mathrm{MPa}$  combined with good ductility and impact toughness.

In order to be able to design appropriate thermo-mechanically controlled rolling processes for the Q&P steels, it is important to characterise the recrystallization behaviour based on the literature information, such as data in our previous studies, among others [14–19]. Semi-empirical relationships have been commonly applied to describe the static recrystallization (SRX) rates of metals and alloys since Sellars and Whiteman [20] and Sellars [21] first presented equations including the process variables strain ( $\varepsilon$ ), strain rate ( $\dot{\varepsilon}$ ) and temperature, and the material variables composition and grain size. Generally, the time for 50% recrystallized fraction ( $t_{50}$ ) can be described by the following empirical relation [20, 21]:

$$t_{50} = A \, \varepsilon^p \, \dot{\varepsilon}^q \, d^s \exp \left( Q_{\rm app} / RT \right) \tag{1}$$

where A is a material constant,  $\varepsilon$  is strain,  $\dot{\varepsilon}$  is strain rate,  $Q_{\rm app}$  is the apparent activation energy of recrystallization, d is grain size, R is the gas constant and T is absolute tem-

perature. The material dependent constants p, q and s describe the powers of strain, strain rate and the grain size, respectively. Using  $t_{50}$  in combination with an Avrami-type equation, the recrystallized fraction can be predicted as a function of temperature and time.

Many regression equations for SRX that have been determined over the years are listed e.g., by Kwon [22], Li et al. [23] and Lenard et al. [24] Unfortunately, most of them are only valid for the specific steel grade used in the experiments so that any quantitative effect of separate alloying elements is difficult to determine from these equations.

Somani et al. [15–19] developed a unique linear regression model to predict the activation energy (Orex) and kinetics of static recrystallization (SRX) for hot-deformed austenite based on the stress relaxation test results of over 40 different carbon steels. The model is able to predict satisfactorily the SRX kinetics of common carbon steel grades including microalloyed steels and also several special steel grades. In the course of the development of this model, the influence of alloying with Mn in the range 0.02-2% and Si up to 1.5% alloying was also considered by including the instances of a couple of dual-phase and TRIP steels. Data for the SRX of high-Mn twinning induced plasticity (TWIP) type austenitic steels have been published [25, 26], but very little SRX data are available for medium-Mn (3-5% Mn) steels apart from the data of Grajcar et al. [27, 28] for 3 %Mn-Al(-Nb) and 5 %Mn-Al(-Nb) steels and Cabanas et al. [29] for binary Fe–Mn alloys. Medina and Mancilla [30] and Medina and Quispe [31] earlier determined the kinetics as a function of chemical composition accounting for the effects of Si and Mn in addition to the microalloying elements of Nb, Ti and V. Increasing Si up to 0.4% in some TRIP steels was found to decrease the SRX rate and increase the activation energy of recrystallization  $(Q_{rex})$  [15, 16] Suikkanen et al. [32] showed that increasing Si beyond 0.4% up to 1.5% has only a small retarding effect on SRX, i.e. the influence of Si appeared to saturate towards 1.5%.

In this study, the SRX characteristics of two Si-alloyed Q&P steels with the compositions (in wt.%) 0.3C-2Mn-1Cr-1Si and 0.25C-3Mn-1.5Si were evaluated and kinetics modelled using a fractional softening approach together with metallography to determine the time for 50% recrystallization as a function of strain, strain rate, grain size and temperature by applying SRX tests using a Gleeble 3800 thermomechanical simulator. SRX fractional softening equations were developed including the determination of strain and strain rate exponents and the activation energy of recrystallization, in accordance with the regression modelling performed previously by Somani et al. [15, 16] for various steels. Some examples of verification of the regression equations and comparisons with other steels including C-Mn, Nb-microalloyed, austenitic stainless steel and TWIP steels are also presented.

Table 1. Chemical compositions of the high-Si Q&P steels. (Fe balance; wt.%).

Steel code	С	Si	Mn	Al	Cr	Mo	Ni	<i>A</i> <sub>3</sub> (°C)	<i>A</i> <sub>4</sub> (°C)
2Mn-1Si	0.296	0.985	1.86	0.0073	1.01	0.002	0.0034	786	1432
3Mn-1.5Si	0.25	1.45	2.91	0.024	0.01	0.002	0.0044	827	1 422

### 2. Experimental procedures

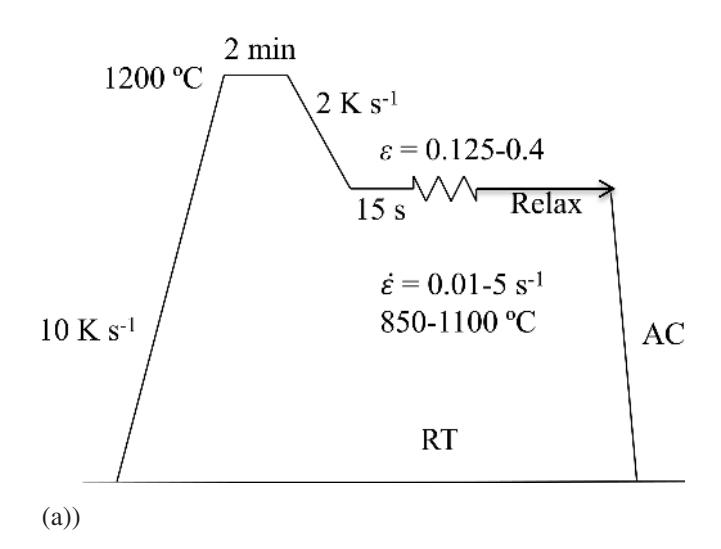
### 2.1. Approach and materials

Two Si-alloyed C–Mn steels intended for Q&P processing were used as experimental materials. The analysed chemical compositions of the two steels, measured using hot rolled samples, are given in Table 1. While one of the high-Si steel compositions, coded 2Mn-1Si, was cast as a 70 kg slab, the other steel, coded 3Mn-1.5Si, was received in the form of a homogenized and hot rolled 11 mm thick plate. Both were procured from OCAS, Belgium. The 2Mn-1Si steel casting was cut into two halves along the mid-thickness in order to circumvent the problem of centreline segregation. A  $200\times80\times60$  mm piece of this casting was soaked at  $1200\,^{\circ}\text{C}$  for 2 h and hot rolled to a 11.2 mm thick plate.  $11\times10$  mm rods cut from the 3Mn-1.5Si plate were given a homogenization treatment in a furnace at  $1250\,^{\circ}\text{C}$  for 2 h prior to preparing the specimens for stress relaxation testing.

Ø 8 mm × 10 mm cylindrical specimens for axisymmetric compression and stress relaxation testing were machined from the two steel plates with the axis of the cylinders transverse to the rolling direction in the rolling plane. The tests were carried out in a Gleeble 3800 thermomechanical simulator. A graphite foil was used as lubricant between the specimen and the tungsten carbide anvils and a tantalum foil to prevent sticking.

### 2.2. Stress relaxation tests

The specimens were heated at a rate of 10 K s<sup>-1</sup> to the reheating temperature 1200 °C and 1250 °C for 2Mn-1Si and 3Mn-1.5Si steels, respectively, held for 2 min, followed by cooling at 2 K s<sup>-1</sup> to the deformation temperature and then compressed up to a prescribed strain after stabilizing the temperature for 15 s at the deformation temperature. The idea of using the higher reheating temperature for 3Mn-1.5Si steel was to provide further homogenization of any Mn-rich segregation bands as far as possible, though the sample was homogenized prior to hot rolling at OCAS, Belgium. Using the stroke mode, the strain was held constant after the deformation while the compressive force relaxed



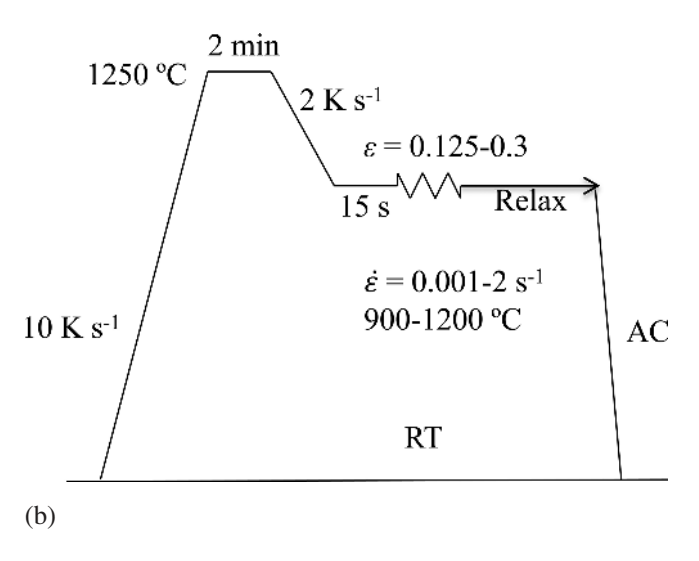


Fig. 1. Test schedules used in stress relaxation tests of (a) 2Mn-1Si, and (b) 3Mn-1.5Si steels. (Abbreviations: RT = room temperature; AC = air cool; Relax = stress relaxation stage).

Table 2. Stress relaxation rest schedules for the experimental high-Si Q&P steels.

Steel	Reheating conditions Temp.(°C)/Time (min)	Grain size (μm)	Test temp. (°C)	Strain	Strain rate (s <sup>-1</sup> )
2Mn-1Si	1 200/2	115	850–1100	0.2	0.1
	1 200/2	115	1 000	0.125-0.4	0.1
	1 200/2	115	1 000	0.2	0.01-5
	1 150/2	80	1 000	0.2	0.1
	1 250/10	400	1 000	0.2	0.1
3Mn-1.5Si	1 250/2	480	900-1200	0.2	0.1
	1 250/2	480	1050	0.125-0.3	0.1
	1 250/2	480	1050	0.2	0.001-2
	1 200/2	80	1 050	0.2	0.1
	1 200/2	80	1 050	0.2	1

in the course of time. The stress relaxation data were then fitted to the Avrami-type (JMAK) equation at around 50% recrystallization to enable an estimation of the SRX fraction as a function of holding time *t*:

$$X = 1 - \exp[-0.693 \cdot (t/t_{50})^n]$$
 (2)

where  $t_{50}$  is the time for 50% recrystallization, which is dependent on the composition of the steel and the deformation conditions, and *n* is the Avrami exponent. In this way, a single experiment can give a complete curve showing recrystallized fraction vs. time for a given set of conditions [33-35]. Stress relaxation tests were carried out in the temperature range 850-1100°C and 900-1200°C for 2Mn-1Si and 3Mn-1.5Si steels, respectively. Table 1 also contains the equilibrium  $A_3$  and  $A_4$  temperatures for the two steel compositions as calculated using Thermo-Calc® software in combination with the TCFE7 database. These demonstrate that all the austenitization treatments as well as deformation and relaxation tests used in this work are in the austenite phase. Both the strain and strain rate were suitably varied at specific temperatures in order to achieve a broad range of deformation parameters for evaluating the SRX characteristics of the two steels. For the 2Mn-1Si steel, these were strain range 0.125-0.4 and strain rates 0.01-5 s<sup>-1</sup> at 1000 °C, and for the 3Mn-1.5Si: 0.125–0.3, 0.001– $2~s^{-1}$  at  $1050\,^{\circ}$ C. Typical test schedules for the two steels are shown in Fig. 1a and b and the details of the experiments are presented in Table 2.

Austenite grain size was measured using the linear intercept method on specimens directly quenched from the reheating temperature with a water spray and etched in saturated picral/teepol solution. Segregation bands, presumably Mn-rich regions, were noticed in the 3Mn-1.5Si steel, despite the homogenization treatment given prior to hot rolling and also reheating at a higher temperature (1250°C) in the Gleeble simulator. Even the 2Mn-1Si steel showed some segregation bands signifying the inadequacy of soaking at 1200°C prior to rolling and subsequent reheating at this temperature.

As seen from Table 2, some specimens were reheated at different reheating temperatures prior to stress relaxation

testing in order to produce relatively coarser or finer grain structures in order to help understand the influence of grain size on SRX kinetics and check the validity of the empirical equations for fractional softening. In addition to the tests listed in Table 2, confirmation tests were also carried out by varying the deformation parameters (strain, strain rate and temperature) randomly to validate the fractional softening equations developed for the two high-Si steels, as discussed later.

### 3. Results and discussion

### 3.1. Flow stress behaviour

Examples of typical true stress – true strain curves obtained on the 2Mn-1Si and 3Mn-1.5Si steels compressed prior to stress relaxation to a true strain of  $\sim 0.2$  at a constant true strain rate of 0.1 s<sup>-1</sup> in the temperature range 850–1100 °C and 900-1200°C respectively, are shown in Fig. 2. The flow stress behaviour displayed the presence of work hardening and dynamic recovery at all deformation temperatures. Hence, subsequent relaxation following hot compression should exhibit static restoration (recovery and recrystallization) processes, except presumably at 1 100 °C in the case of 2Mn-1Si steel (Fig. 2a) and at 1150-1200°C in the case of 3Mn-1.5Si (Fig. 2b) steels, where the critical strain for the initiation of dynamic recrystallization (DRX)  $\varepsilon_c$  might be exceeded ( $\varepsilon_c$  is about 0.8 times peak strain  $\varepsilon_p$  [21, 36]). The peak strain was, however, not determined. In these cases, the conditions are perhaps at the borderline between static and metadynamic (MDRX) recrystallization. Similarly, the flow stress behaviour of samples tested at higher strains and lower strain rates were carefully examined to identify the test conditions where deformation exceeded, or might have exceeded, the critical strain ( $\varepsilon_c$ ), in order to exclude these cases from the modelling of the fractional softening equations for SRX.

Comparing the flow stress levels, it seems that there are no significant differences between the two steels. Similar observations were made for 3 %Mn and 5 %Mn steels tested

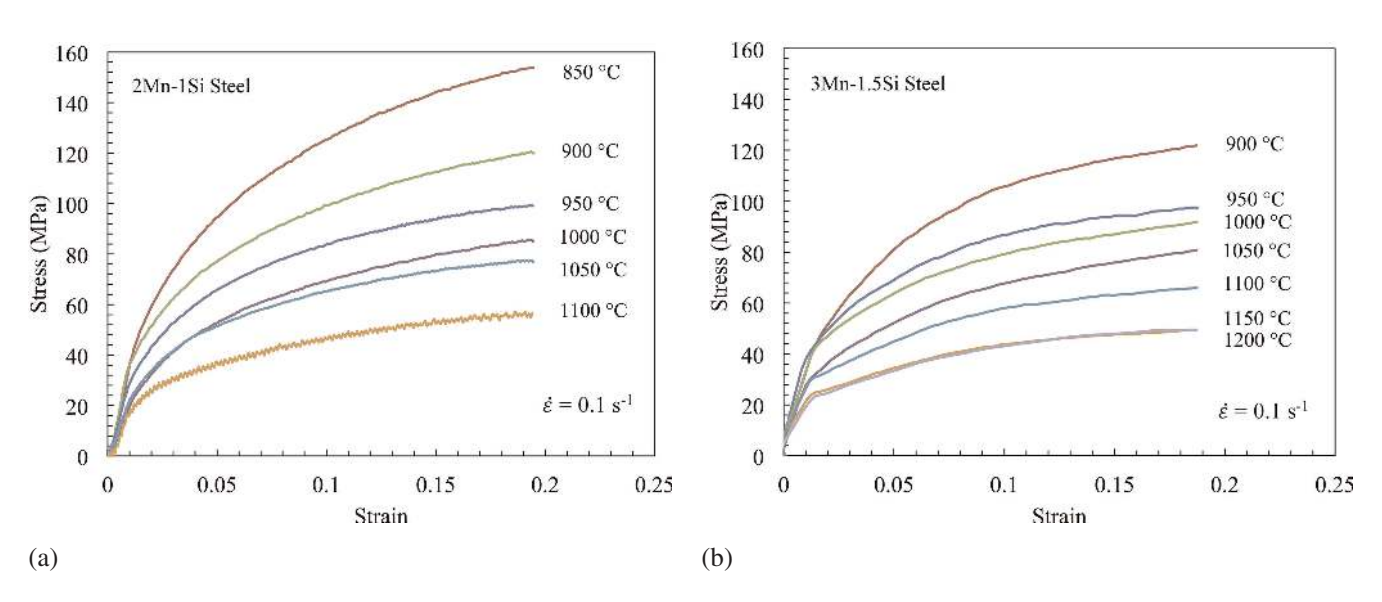


Fig. 2. True stress – true strain curves following hot compression to 0.2 strain at  $0.1 \text{ s}^{-1}$  in the temperature ranges  $850-1100 ^{\circ}\text{C}$  and  $900-1200 ^{\circ}\text{C}$  for (a) 2Mn-1Si, and (b) 3 Mn-1.5 Si steels, respectively, revealing work hardening and dynamic recovery behaviour.

at the strain rate of  $0.1~\rm s^{-1}$  in the range  $850{\text -}1150\,^{\circ}{\rm C}$  by Grajcar et al. [27, 28], who found no effect of Mn on the flow stress behaviour. They observed the peak strain at  $1150\,^{\circ}{\rm C}$  to be about 0.25.

### 3.2. Stress relaxation behaviour

Examples of typical stress relaxation curves for the two steels, recorded during 600 or 1000 s, corresponding to the compression tests shown in Fig. 2a and b, are presented in Fig. 3a and b. In this instance, the stress relaxation curves are quite flat, but they display essentially three stages on the logarithmic time scale. It has been presented earlier that the initial and final linear stages on the stress relaxation curves correspond to the occurrence of static recovery and the intermediate faster drop in the stress level indicates the SRX or MDRX process [33-35]. Stress relaxation curves were carefully analysed to determine the kinetics of the SRX process as a function of deformation parameters. The degree of softening at a given time can be determined from recrystallized fraction vs. time curves computed from the stress relaxation data. Examples of these curves fitted with the sigmoidal Avrami-type curves are shown in Fig. 4a and b, illustrating the effect of temperature on the kinetics of SRX, for instance. More details and analysis of experimental parameters on the SRX kinetics are discussed in subsequent sections.

### 3.3. Effect of temperature and grain size on SRX rate

Referring to Fig. 3a, the stress relaxation curves of the 2Mn-1Si steel reveal the influence of temperature on the SRX kinetics after deformation to 0.2 strain at 0.1 s<sup>-1</sup> at different temperatures in the range 900 °C to 1100 °C in steps of 50 °C. It can be seen that with an increase in temperature from 850 °C to 1100 °C, the SRX rate increases signifi-

cantly. Complete softening was obtained in most cases, except at the lower temperatures ( $\leq 900\,^{\circ}$ C). At 850 °C, the final flow stress remained clearly higher than for the other temperatures indicating a lack of recrystallization. The effect of temperature on the Avrami exponent is quite distinct; it varies from 1.0 at lower temperatures (900–1000 °C) to 1.4 at higher temperatures (1050–1100 °C). The time for 50% recrystallization,  $t_{50}$ , decreases from 68 s at 900 °C to about 3.7 s at 1100 °C, Fig. 4a. So far as the influence of grain size is concerned, stress relaxation data obtained on specimens reheated 10 min at 1250 °C (Table 2) to produce coarse grains ( $\sim 400\,\mu\text{m}$ ) and tested at  $1000\,^{\circ}\text{C}/0.2/0.1\,\text{s}^{-1}$  clearly revealed the retardation of SRX rate ( $t_{50} = 24\,\text{s}$ ) in comparison to that of the finergrained structure (115  $\mu\text{m}$ ;  $t_{50} = 13\,\text{s}$ ).

The stress relaxation curves for the 3Mn-1.5 Si steel, as presented in Fig. 3b, show that the SRX rate increases with increasing temperature and the softening was complete in most cases. However, the flow stress remained relatively high at the lowest temperature of 900 °C, indicating incomplete recrystallization in the time span used. Unlike in the case of the 2Mn-1Si steel, the Avrami exponent varied in a narrow range between 1.3-1.5 (mostly 1.4) irrespective of the test temperature, as can also be discerned from the nearly parallel Avrami curves fitting the relaxation data (Fig. 4b). The time  $t_{50}$  increases from 2.1 s at 1150 °C to about 37 s at 950 °C. The effect of grain size on SRX kinetics was evaluated by including a finer grain structure (80 µm) obtained by reheating at a somewhat lower temperature of 1200°C for 2 min prior to compression at 1050 °C to 0.2 strain at 0.1 s<sup>-1</sup> (Table 2). The corresponding acceleration of the recrystallization rate ( $t_{50} = 2.6 \text{ s}$ ) in comparison with that of the coarse-grained structure (480  $\mu$ m;  $t_{50}$  = 12 s) further confirmed the significant influence of grain size on the SRX rate.

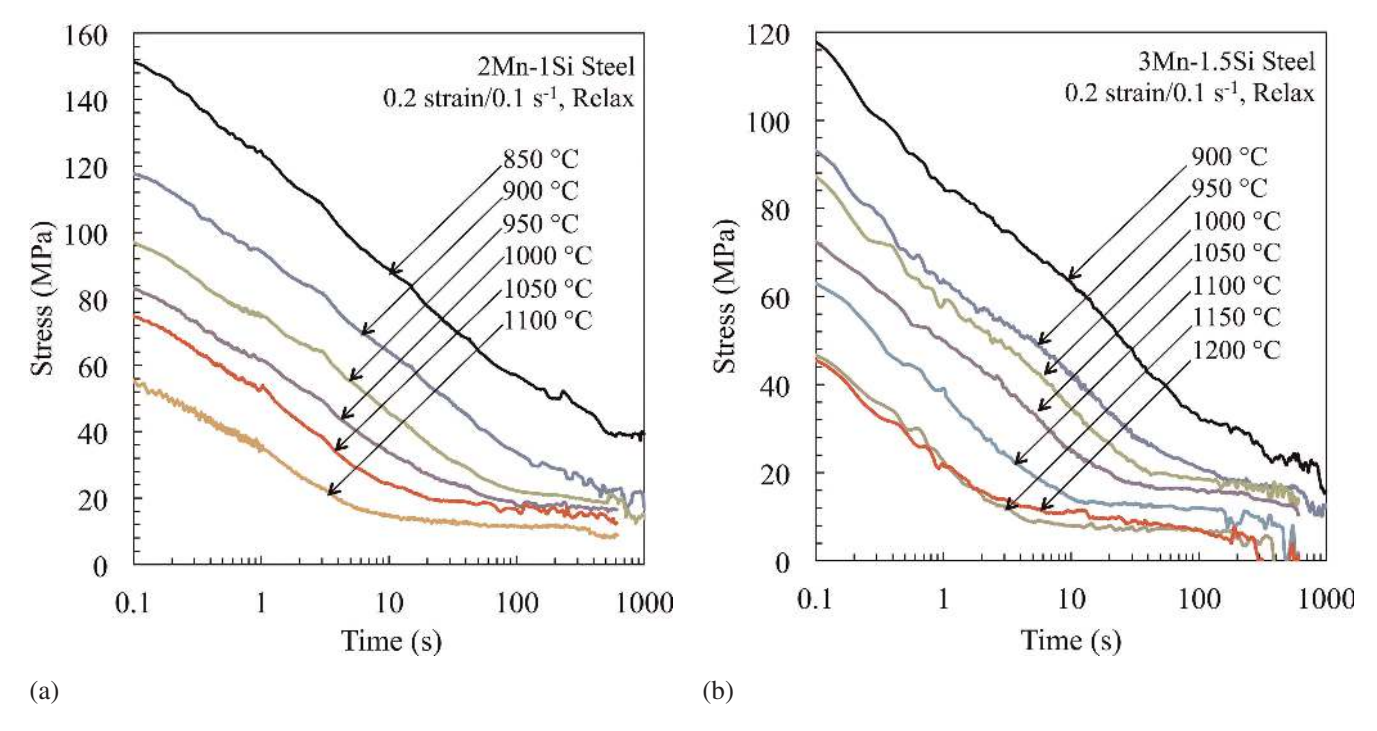


Fig. 3. Typical stress relaxation curves obtained on specimens deformed to a true strain of 0.2 at 0.1 s<sup>-1</sup>: (a) 2Mn-1Si, and (b) 3Mn-1.5Si steels.

### 3.4. Apparent activation energy of recrystallization $(Q_{app})$

The temperature dependence of the SRX kinetics for the 2Mn-1Si and 3Mn-1.5Si steels are shown in Fig. 5a and b, where the times for 5%, 50% and 95% recrystallization  $(t_5, t_{50})$  and  $t_{95}$  respectively) are plotted against the inverse absolute temperature. The times were estimated at different temperatures for specimens deformed to 0.2 strain at 0.1 s<sup>-1</sup> based on both the relaxation data and corresponding Avrami type fits at about 50% recrystallization. As seen from Fig. 5a, the data at 50 % recrystallization ( $t_{50}$ ) and the effective end of recrystallization ( $t_{95}$ ) are reasonable, but there is a scatter in the start of the recrystallization  $(t_5)$ , as is also apparent in the relaxation curves (Fig. 3a). The slope of the  $t_{50}$ data plotted vs. the inverse absolute temperature (1/T) was used in estimating the apparent activation energy for recrystallization ( $Q_{app}$ ). When doing this, the cases of incomplete recrystallization (at low temperatures) and MDRX (at high temperatures) were carefully excluded. As explained in a publication of Karjalainen [33], it can be concluded that recrystallization is only partial, if the stress relaxation curve is still declining in the final stage of the test or if it remains at a relatively high stress level for the temperature concerned. In Fig. 3 it is seen that the relaxation curves approach each other at all temperatures other than 850 °C (Fig. 3a) and perhaps at 900 °C (Fig. 3b). On the other hand, the data for 1100 °C and 1150-1200 °C for the 2Mn-1Si and 3Mn-1.5Si steels, respectively, were not included in the analysis because of the possibility of MDRX. The estimated  $Q_{\rm app}$  values for the 2Mn-1Si and 3Mn-1.5Si steels were about 225 and 241 kJ mol<sup>-1</sup>, suggesting that an increase in Si and Mn contents increases  $Q_{\rm app}$ .

Mn contents increases  $Q_{\rm app}$ . The observed  $Q_{\rm app}$  values for the two steels fall in the 177–283 kJ mol<sup>-1</sup> range of values reported for other steels, i.e. for C–Mn 184 kJ mol<sup>-1</sup> [15, 16], 9SMn28 free cutting steel 177 kJ/mol [37], 0.2C-2Mn-0.6Cr-(0-1.5)Si 193–227 kJ mol<sup>-1</sup> [32], C–Mn–Nb 230 kJ mol<sup>-1</sup> [15, 16], 12Cr stainless 265 kJ mol<sup>-1</sup> [38], ordinary Fe-20Mn-1.5Al TWIP

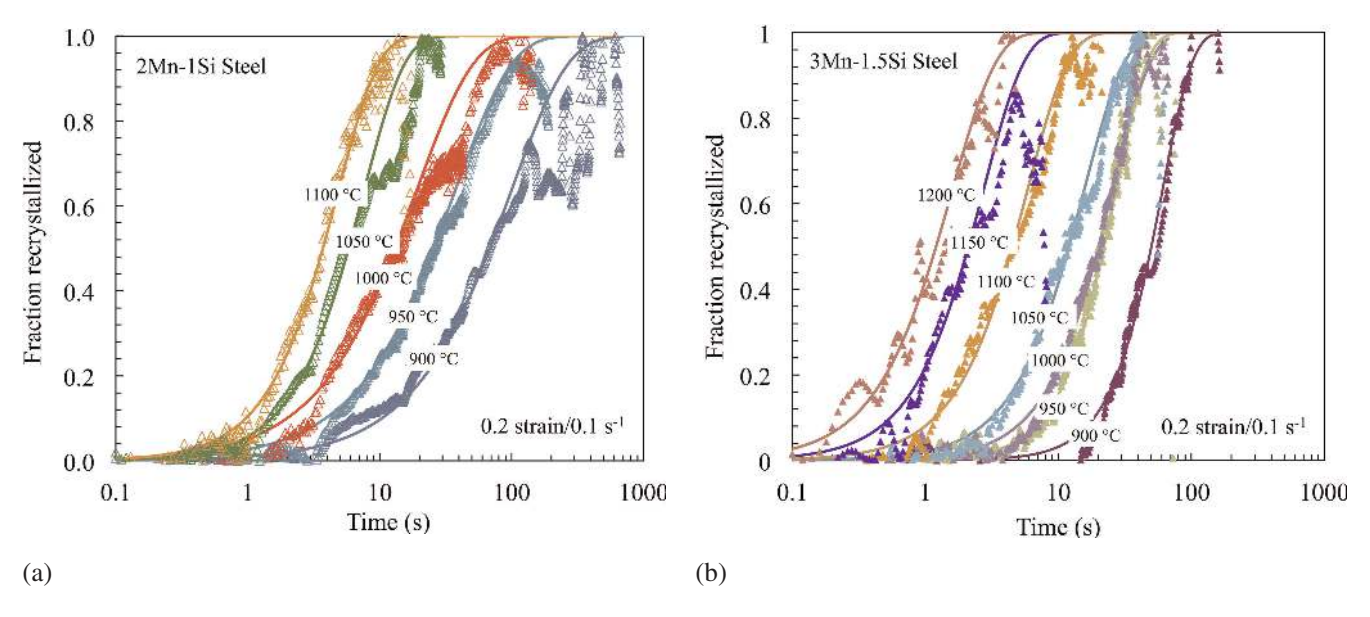


Fig. 4. Fraction recrystallized vs. time data fitted with Avrami type curves for (a) 2Mn-1Si and (b) 3Mn-1.5Si steels.

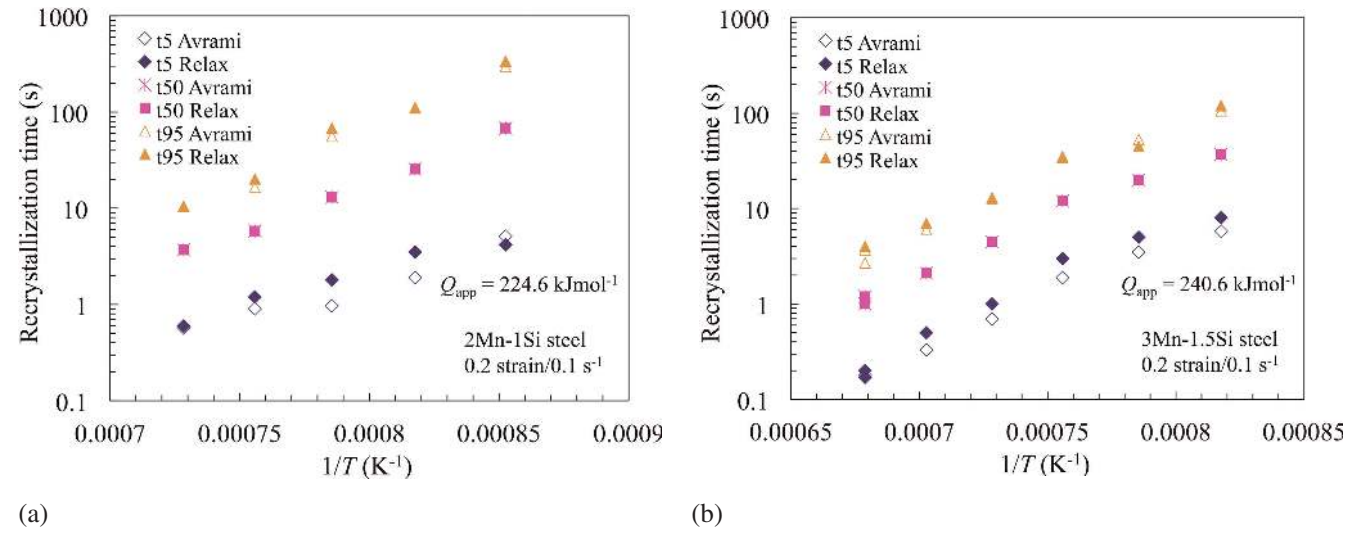


Fig. 5. Estimation of  $Q_{\rm app}$  for the SRX process: (a) 2Mn-1Si steel, and (b) 3Mn-1.5Si steel.

218 kJ  $\,$  mol $^{-1}$  and Nb-microalloyed Fe-20Mn-1.5Al-0.026Nb TWIP steel 273 kJ  $\,$ mol $^{-1}$  [26] and Type 304 stainless steel 283 kJ  $\,$ mol $^{-1}$  [38].

### 3.5. Powers of strain and strain rate

The effects of strain and strain rate on  $t_{50}$  times for the two steels are displayed in Fig. 6a and b. The powers of strain (p) and strain rate (q) have been estimated based on the plots of (i)  $t_{50}$  vs. strain at 0.1 s<sup>-1</sup> and a given temperature  $1\,000\,^{\circ}\mathrm{C}$  and  $1\,050\,^{\circ}\mathrm{C}$  for the 2Mn-1Si and 3Mn-1.5Si steels, respectively) (Fig. 6a), and (ii)  $t_{50}$  vs. strain rate following compression to 0.2 strain at the deformation temperature (Fig. 6b).

As can be discerned from Fig. 6a, the slopes of the line fits are fairly reasonable despite some scatter and the corresponding powers of strain (p) were estimated to be about -2.8 and -2.35 for the 2Mn-1Si and 3Mn-1.5 Si steels, respectively. The power of strain (p) for the 3Mn-1.5Si steel (-2.35) is slightly lower than that of 2Mn-1.5Si (-2.8). The strain exponent for C-Mn steels has been reported to be in the range -2.5 to -4 [14-19, 39, 40]. Values between -2 and -3 were measured by the stress relaxation technique for some microalloyed steels [14-16, 35, 41]. Values of -2.8 and -2.5 for the strain exponent have been used by Somani et al. [15, 16, 19] for C/C-Mn/Nb/Ti/Nb-Ti and Mn-V steels, respectively. Lang et al. [42] and Suikkanen et al. [32] obtained a value of -2.1 for p in the case of a 0.2C-2.0Mn-1.48Si-0.6Cr steel. Hence, all these values are of the same order and any distinct dependence on alloying can hardly be seen.

Similarly, the slopes of the line fits in Fig. 6b show the powers of strain rate (q) to be -0.23 and -0.14 for the 2Mn-1Si and 3Mn-1.5 Si steels, respectively. The limited data for 0.1C-1.2Mn-1.15 Si steel has been included in

Fig. 6b for comparison [16]. It gives the same power of strain rate (-0.23) as that of the 2Mn-1.5Si steel. Lang et al. [42] determined the SRX kinetics for a 0.21C-1.48Si-2.04Mn-0.6Cr composition, also tested by Suikkanen et al. [32], and found q to be -0.18. It is noteworthy that the 2Mn-1.5Si steel contains 1% Cr in solution, and the steel studied by Lang et al. [42] and Suikkanen et al. [32] contained 0.6% Cr. The Cr alloying, however, might not have any significant influence on the power of strain rate (nor the power of strain), as Cr (like Ni) in low concentrations has hardly shown any discernible influence on the SRX kinetics of C-Mn steels [15–17]. Also, lower values of q of -0.11 and -0.12 have been reported for C/C-Mn and Ti-microalloyed steels, respectively [14–16, 19, 43]. For Nb and Nb–Ti and also Mo-steels, q has been estimated to be of the order of -0.23 [15, 16, 19]. In summary, all these values of q fall within a reasonably narrow range (-0.11 to -0.23) indicating a weak dependence of SRX on strain rate irrespective of the steel alloying.

### 3.6. Effect of Si and Mn on $Q_{\text{rex}}$

The activation energy of SRX ( $Q_{\rm rex}$ ) is dependent on the  $Q_{\rm app}$ , the power of strain rate q, and the activation energy of deformation  $Q_{\rm def}$ . Somani et al. [15–18] adopted the  $Q_{\rm def}$  of 340 kJ mol<sup>-1</sup> for C–Mn steels in the development of the regression model for the  $Q_{\rm rex}$  in hot deformed austenite. In good agreement, Suikkanen et al. [32] reported  $Q_{\rm def}$  values increasing in the range 324 to 353 kJ mol<sup>-1</sup> for 0.2C-2.0Mn-0.6Cr-Si steels with Si content increasing from 0.04 to 1.48%. The influence of Si was not linear, however, as an increase in Si content from 1.0 to 1.5% only changed  $Q_{\rm def}$  from 348 to 353 kJ mol<sup>-1</sup>, i.e. by only 5 kJ mol<sup>-1</sup>. Cabanas et al. [29] determined  $Q_{\rm def}$  values for various Fe–Mn binary alloys and reported that Mn generally caused an in-

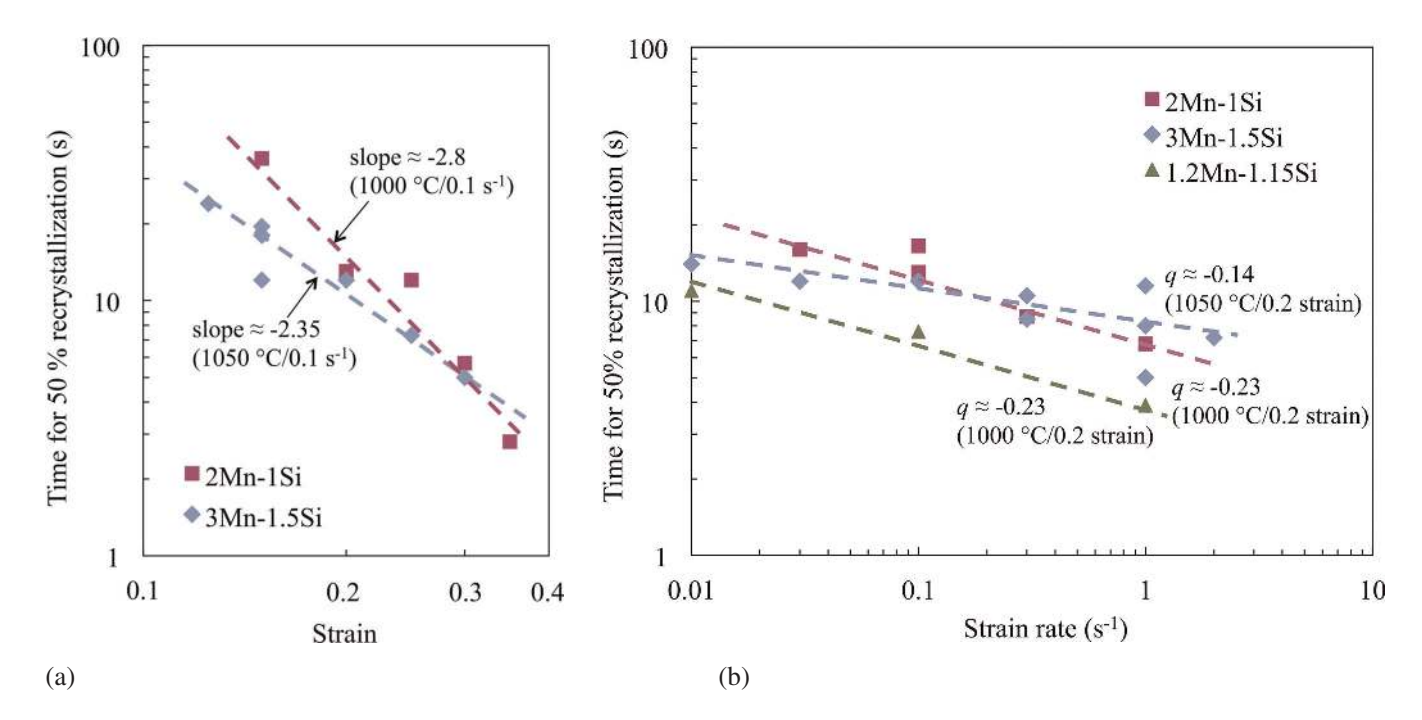


Fig. 6. (a) Dependence of  $t_{50}$  on strain in the SRX (<0.35 strain) regime for 2Mn-1Si and 3Mn-1.5 Si steels deformed at  $1\,000\,^{\circ}$ C/0.1 s<sup>-1</sup> and  $1\,050\,^{\circ}$ C/0.1 s<sup>-1</sup>, respectively, and (b) estimation of the power of strain rate for the two steels deformed to 0.2 strain in the SRX regime. Data for 0.1C-1.2Mn-1.15Si steel [16] is also included in Fig. 6b for comparison.

crease of  $Q_{\rm def}$  at Mn contents below 10%. However, the maximum  $Q_{\rm def}$  of 350 kJ mol<sup>-1</sup> was measured for an Fe-3%Mn alloy.

Using a constant  $Q_{\rm def}$  of 340 kJ mol<sup>-1</sup> for both the 2Mn-1Si and 3Mn-1.5Si steels gives  $Q_{\rm rex}$  values of 303 and 289 kJ mol<sup>-1</sup>, respectively. The low value of  $Q_{\rm rex}$  for the 3Mn-1.5Si steel results from its less negative q (–0.14 as opposed to –0.23), even though its  $Q_{\rm app}$  was higher than that of the 2Mn-1Si steel, as expected from its higher alloy content.

A linear regression analysis [15–18] showed that  $Q_{\rm rex}$  for C–Mn and microalloyed steels is given by:

$$Q_{\text{rex}}(kJ \text{ mol}^{-1}) = 3803CF + 109418 \tag{3}$$

Here CF, the composition factor, is given by:

$$CF = 2Cr + 10 = Cu + 15Mn + 50Mo + 60Si + 70V$$
  
+230Ti + 700Nb (4)

where the elements are in wt.% and the effects of Si and Nb are considered to saturate at 0.4% Si and 0.044% Nb. These equations lead to  $Q_{\rm rex}$  values of 314 and 366 kJ mol<sup>-1</sup> respectively for the 2Mn-1Si and 3Mn-1.5Si steels. The former value is only marginally higher than the experimental value 303 kJ mol<sup>-1</sup>, but for the 3Mn-1.5Si steel the model prediction far exceeds the experimentally observed value of 289 kJ mol<sup>-1</sup>. This suggests that the regression model breaks down here perhaps due to a saturation in the effect of Mn on CF at concentrations beyond the 2%, which was the highest Mn content of the steels used to develop the regression equation above. Assuming such a saturation effect, the above equations would predict essentially the same  $Q_{\rm rex}$  values for both steels,  $\sim 315$  kJ mol<sup>-1</sup>.

In a study of Karjalainen et al. [44], two TRIP steels 1.15Mn-1.1Si and 1.5Mn-1.5Si were tested as well as several C–Mn steels with lower Si contents. The experimental

 $Q_{\rm rex}$  values determined were 240 and 275 kJ mol<sup>-1</sup> for those two 1.15Mn-1.1Si and 1.5Mn-1.5Si steels, respectively [44]. Based on the data for the C–Mn–Si steels with Mn < 2%, it was suggested that the effect of Mn on  $Q_{\rm rex}$  is low in comparison to Si and that the entire data could be approximately fitted with a logarithmic dependence of  $Q_{\rm rex}$  on the Si concentration, namely  $Q_{\rm rex}({\rm kJ~mol^{-1}})$  = 260 + 26.7ln(wt.%Si).

Suikkanen et al. [32] reported  $Q_{\text{rex}}$  values between 229 and 291 kJ mol<sup>-1</sup> for a 0.2C-2.0Mn-0.6Cr-Si steel with the Si contents varying between 0.04 and 1.48%. They also pointed out that the influence of Si seems to saturate towards the higher contents, increasing more slowly beyond about 0.5 % Si. The saturating tendency is consistent with our previous observations on the influence of Si concentration suggesting that beyond a certain level, an element may lose its efficiency to retard recrystallization any further, presumably due to occupation of lattice sites at the moving grain boundaries leading to a saturation of the solute drag effect [16]. According to the work of Suikkanen et al. [32], an increase in Si content from 1.08 to 1.48% will raise  $Q_{\text{rex}}$  by about 6 kJ mol<sup>-1</sup>. Ignoring any possible effects of other alloying elements, this is the difference in  $Q_{\text{rex}}$  expected between the 2Mn-1Si and 3Mn-1.5Si. The measured difference is marginally negative at -14 kJ mol<sup>-1</sup>, however.

### 3.7. Fractional softening equations for SRX

The power of grain size described by the relation  $s = 2.13d^{-0.105}$  has been previously determined based on measured SRX data for a large number of carbon steels, with and without microalloying [15, 16]. Hence, it has now been extended to the current high-Si 2–3% Mn steels, too. Taking the power of grain size to be described by the above relation, together with the above values for the other parameters ( $Q_{app}$ , p and q) in Eq. 1 gives the constant A for the two

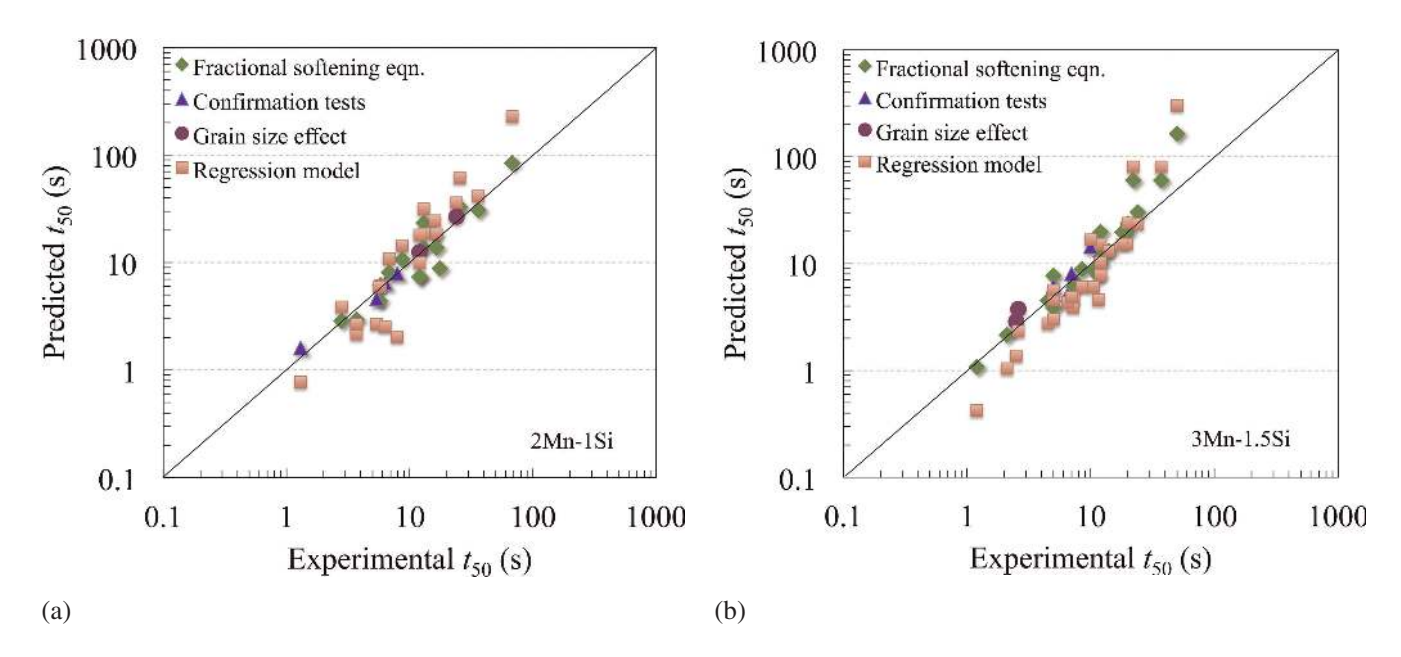


Fig. 7. Plots of predicted vs. experimental  $t_{50}$  data for (a) 2Mn-1Si, and (b) 3Mn-1.5Si steels. The diamond, triangle and circle symbols represent predictions obtained using Eqs. (5) and (6), which are based on the diamond data points. The square points are obtained using the regression model [15–19].

steels. The SRX rate, therefore, can be reasonably described by the following SRX equations:

2Mn-1Si steel: 
$$t_{50} = 1.17 \times 10^{-13} \,\varepsilon^{-2.8} \,\dot{\varepsilon}^{-0.23} \,d^s$$
  
 $\exp(224600/RT)$  (5)

3Mn-1.5Si steel: 
$$t_{50} = 5.73 \times 10^{-14} \,\varepsilon^{-2.35} \,\dot{\varepsilon}^{-0.14} \,d^s$$
  
exp(240600/RT) (6)

In order to check the reliability of the fractional softening equation (Eq. (5)) derived for the 2Mn-1Si steel, a few confirmation experiments were carried out by randomly varying the deformation parameters, (for example, 1075 °C/0.17/0.5  $s^{-1}$ , 1025 °C/0.25/0.3  $s^{-1}$ , etc.) and/or using a coarse or fine grain size (400 or 80 µm; see Table 2) followed by deformation at 1000 °C to 0.2 strain at 0.1 s<sup>-1</sup>. Figure 7a presents examples of the plots of experimental vs. predicted  $t_{50}$  values for all deformation conditions. Data from confirmation tests for validation are also included in the figure. It can be seen that the agreement between the experimental and predicted values (pred/exp ratio in the range 0.79-1.29) is quite satisfactory, except for one test at 1000 °C/0.01 s<sup>-1</sup>, which shows nearly half the predicted  $t_{50}$  value (pred/exp ratio: 1.8). This indicates that the above fractional softening equation gives a reasonable prediction of the SRX kinetics for the 2Mn-1Si steel. Also, the equation describing the power of grain size (s) was found to be reasonable for this steel, too.

Confirmation experiments were also carried out for the 3Mn-1.5Si steel by varying the deformation parameters, such as 1025 °C/0.3/0.07 s<sup>-1</sup>, 1075 °C/0.175/0.3 s<sup>-1</sup>, etc. and also, using a fine grain size (80 µm; see Table 2) followed by deformation to a strain of 0.2 at 1050 °C at two different strain rates (0.1 and 1 s<sup>-1</sup>). Figure 7(b) presents the plots of experimental vs. predicted  $t_{50}$  values for all deformation conditions, in addition to the data from confirmation tests. The figure suggests that the agreement between the experimental and predicted data (pred/exp ratio in the range 0.78–1.65) is satisfactory, except for one test at 950 °C, which shows nearly one-third the predicted  $t_{50}$  value (pred/exp ratio: 2.73). Anyhow, the equation describing the power of grain size (s) was found to be acceptable for this steel, too. Thus, the fractional softening equations (Eqs. (5) & (6)) developed for the two steels are reasonable and the equations can be used in designing the industrial rolling scheme during thermo-mechanical processing prior to quenching and partitioning.

The predictions resulting from the previously developed regression model are also included in Fig. 7a and b. It can be seen that the model predictions are acceptable for both steels, provided an upper saturation limit of 2 % Mn is used when calculating  $Q_{\text{rex}}$  from Eqs. (3) and (4). Despite considering the saturation of the effect of Mn at around 2%, it is also possible that the effect of Mn is non-linear, with a maximum retardation effect at some intermediate concentration between 2 and 3%. For example, Grajcar et al. [27, 28] observed that increasing Mn content from 3 to 5% accelerated the SRX kinetics. Thus, the effect of Mn on SRX behaviour seems somewhat complex. Notwithstanding these incongruities, the predictions were found to be reasonably good suggesting the usefulness of the model in predicting the SRX kinetics for the 3Mn-1.5 Si steel (Fig. 7b), though the data are somewhat scattered (pred/exp ratio in the range 0.17–2.84; average ratio =  $\sim 1.31$ ; SD = 0.59).

Two experiments (1065 °C/0.215/0.3 s<sup>-1</sup>/3 s relaxation and 940 °C/0.23/0.13 s<sup>-1</sup>/25 s relaxation) were carried out to quench the 2Mn-1Si test specimens in water after relaxing for times corresponding to 50% recrystallized fraction following different deformation conditions, as calculated using Eq. (5). Metallographic analysis, however, was inconclusive because of the difficulties in etching the samples and distinguishing between the strained (unrecrystallized) and recrystallized areas. Attempts to analyze the microstructures using scanning electron microscopy – electron back scatter diffraction (SEM-EBSD) are equally challenging and were not tried in this study. However, validity of the stress relaxation technique in the study of recrystallization has been demonstrated metallographically in our previous studies, c.f. references [14, 38].

### 3.8. Comparison of SRX kinetics of various steel types

The  $t_{50}$  times estimated for the present steels by using the fractional softening equations (Eqs. (5) and (6)) derived above are compared with other steels for a strain of 0.2 at 0.1 s<sup>-1</sup> and a grain size of 140 µm (computed using the relation for s), as shown in Fig. 8. The plots are based on various equations/data generated at the University of Oulu: 304SS [38], Nb-TWIP and TWIP [26], C-Mn-Nb and C-Mn [15, 16]. The SRX kinetics of the present high-Si steels are quite similar despite the different levels of Si and Mn alloying. As expected, C-Mn steel exhibits the fastest SRX rate, while Type 304 stainless steel is the slowest. On the other hand, the SRX kinetics of present high-Si steels have been found to be marginally faster but close to that of 0.03 %Nb-microalloyed C-Mn (C-Mn-Nb) steel as well as an ordinary TWIP steel (Fe-20Mn-1.5Al), but much faster than the SRX rate of a Nb-microalloyed TWIP steel (Fe-20Mn-1.5Al-0.026Nb). Clearly, Nb significantly slows down the rate of SRX in both C-Mn and high-Mn TWIP steels. However, the addition of 1–1.5 % Si in the high-Si steels seems to have a potent effect, but weaker than that of Nb in C-Mn steel and that of high Mn in TWIP steel. Mn, on the other hand, is shown to have a weaker effect on the SRX kinetics of steels compared to that of Si [15, 16, 19]. Cr present in 2Mn-1Si steel might not have any discernible effect on the SRX kinetics, as established earlier during the development of the unique regression model [15-19], but its possible influence on q is yet to be established through further study.

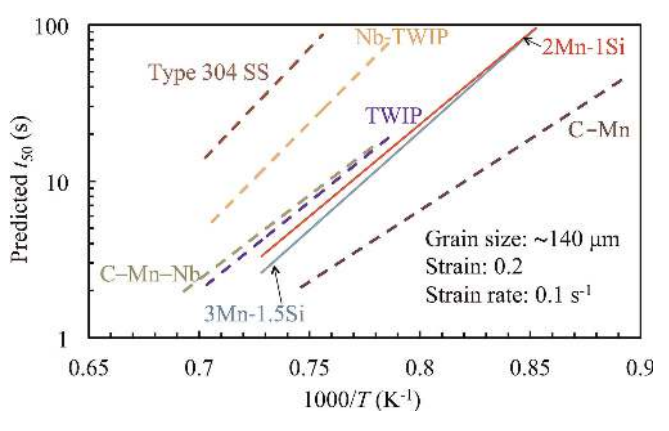


Fig. 8. Plots of  $t_{50}$  vs. inverse absolute temperature for the present high-Si steels in comparison with other steels.

### 4. Summary and conclusions

In this study, the recrystallization characteristics of two experimental high-Si Q&P steels containing 0.25-0.30% C together with 2%Mn-1%Si and 3%Mn-1.5%Si under hot deformation conditions have been evaluated using the stress relaxation technique on a Gleeble 3800 thermomechanical simulator. Deformation temperatures ranged from 850 to 1200 °C, strains from 0.125 to 0.4 and strain rates 0.001 to 5 s<sup>-1</sup>. Initial grain sizes were from 80 to 480  $\mu$ m. For both steels, the time for 50 % recrystallization was exponentially proportional to the inverse of temperature and directly proportional to the product of strain, strain rate and grain size all raised to various powers.

Data analysis resulted in the estimation of the powers of strain (-2.8 and -2.4) and strain rate (-0.23 and -0.14) and the recrystallization activation energies (303 and 289 kJ mol<sup>-1</sup>) for the 2Mn-1Si and 3Mn-1.5Si steels, respectively. This suggests that increasing the contents of Mn and Si made the recrystallization kinetics less sensitive to strain, strain rate and temperature, i.e. the powers of strain and strain rate became less negative and the activation energy of recrystallization was reduced. The power of grain size was the same for both steels, following that found earlier for low-alloy steels.

Equations are given that can be used to predict recrystallization times for the two steels thereby avoiding partial recrystallization and ensuring fine grain sizes during the rough rolling stage of thermomechanical rolling.

An equation developed earlier on the basis of tens of C-Mn and microalloyed steels has been shown to describe the recrystallization times of the present steels with reasonable accuracy if it is assumed that the effect of Mn on the activation energy of recrystallization saturates at the level of

It is shown that the SRX rates of the present steels are typically lower than those of ordinary C-Mn steels, but marginally higher than those of C-Mn-Nb steel and an ordinary TWIP steel (Fe-20Mn-1.5Al).

The funding of this research activity through the RFCS Grant Agreement RFSR-CT-2014-00019 is gratefully acknowledged. Authors would like to thank Mr. Juha Uusitalo for meticulously conducting the Gleeble tests.

### References

- [1] J.G. Speer, D.V. Edmonds, F.C. Rizzo, D.K. Matlock: Curr. Opin. Solid State Mater. Sci. 8 (2004) 219. DOI:10.1016/j.cossms.2004.09.003
- [2] H.Y. Li, X.W. Lu, W.J. Li, X.J. Jin: Metall. Mater. Trans. A 41 (2010) 1284. DOI:10.1007/s11661-010-0184-8
- [3] E. De Moor, S. Lacroix, A.J. Clarke, J. Penning, J.G. Speer: Metall. Mater. Trans. A 39 (2008) 2586. DOI:10.1007/s11661-008-9609-z
- [4] J.G. Speer, F.C.R. Assunção, D.K. Matlock, D.V. Edmonds: Mater. Res. 8 (2005) 417. DOI:10.1590/S1516-14392005000400010
- [5] A.J. Clarke, J.G. Speer, M.K. Miller, R.E. Hackenberg, D.V. Edmonds, D.K. Matlock, F.C. Rizzo, K.D. Clarke, E. De Moor: Acta Mater. 56 (2008) 16. DOI:10.1016/j.actamat.2007.08.051
- [6] D.V. Edmonds, K. He, F.C. Rizzo, B.C. De Cooman, D.K. Matlock, J.G. Speer: Mater. Sci. Eng. A 438-440 (2006) 25. DOI:10.1016/j.msea.2006.02.133
- [7] M.C. Somani, L.P. Karjalainen, D.A. Porter, R.D.K. Misra: Mater. Sci. Forum 706-709 (2012) 2824 DOI:10.4028/www.scientific.net/MSF.706-709.2824

- [8] M.C. Somani, D.A. Porter, L.P. Karjalainen, D.K. Misra: Int. J. Metall. Eng. 2 (2013) 154. DOI:10.5923/j.ijmee.20130202.07
- M.C. Somani, D.A. Porter, L.P. Karjalainen, P.P. Suikkanen, D.K. Misra: Mater. Sci. Forum 783-786 (2014) 1009. DOI:10.4028/www.scientific.net/MSF.783-786.1009
- [10] M.C. Somani, D.A. Porter, L.P. Karjalainen, P.P. Suikkanen, R.D.K. Misra: J. Mater. Today: Proc. 2S (2015) S631. DOI:10.1016/j.matpr.2015.07.363
- [11] M.C. Somani, D.A. Porter, J.I. Kömi, L.P. Karjalainen, D.K. Misra, in: Proc. Int. Symp. New Developments in Advanced High-Strength Sheet Steels, Keystone, AIST, Warrendale, PA (2017) 331.
- [12] X. Tan, Y. Xu, X. Yang, Z. Liu, D. Wu: Mater. Sci. Eng. A 594 (2014) 149. DOI:10.1016/j.msea.2013.11.064
- [13] Z.L. Tang, S.-S. Cao, X.-P. Zhang: Steel Res. Int. 86 (2015) 429. DOI:10.1002/srin.201400244
- [14] J. Perttula: Ph.D. thesis, Physical Simulation of Hot Working: Measurements of Flow Stress and Recrystallization Kinetics, Acta Universitatis Ouluensis Technica, C 119, University of Oulu, Finland (1998).
- [15] L.P. Karjalainen, M.C. Somani, D.A. Porter, R.A. Morgridge, in: M. Pietrzyk, Z. Mitura, J. Kaczmar (Eds.), Proc. The 5th Int. ESA-FORM Conf., Krakow, Poland (2002) 603.
- [16] M.C. Somani, L.P. Karjalainen, D.A. Porter, R.A. Morgridge, in: E.J. Palmiere, M. Mahfouf, C. Pinna (Eds.), Proc. Int. Conf. Thermomechanical Processing: Mechanisms, Microstructure and Control, The University of Sheffield, UK (2003) 436.
- [17] M.C. Somani, L.P. Karjalainen: Mater. Sci. Forum 467-470 (2004) 335. DOI:10.4028/www.scientific.net/MSF.467-470.335
- [18] M.C. Somani, L.P. Karjalainen: Mater. Sci. Forum 550 (2007) 583. DOI:10.4028/www.scientific.net/MSF.550.583
- [19] M.C. Somani, L.P. Karjalainen: Mater. Sci. Forum 715-716 (2012) 751. DOI:10.4028/www.scientific.net/MSF.715-716.751
- [20] C.M. Sellars, J.A. Whiteman: Metal Sci. 13 (1979) 187. DOI:10.1179/msc.1979.13.3-4.187
- [21] C.M. Sellars, in: C.M. Sellars, G. J. Davies (Eds.), Proc. Int. Conf. Hot Working and Forming Processes, The Metals Society, London (1980) 3
- [22] O. Kwon: ISIJ Int. 32 (1992) 350. DOI:10.2355/isijinternational.32.350
- [23] G. Li, T.M. Maccagno, D.Q. Bai, J.J. Jonas: ISIJ Int. 36 (1996) 1479. DOI:10.2355/isijinternational.36.1479
- [24] J.G. Lenard, M. Pietrzyk, I. Cser: Mathematical and Physical Simulation of the Properties of Hot Rolled Products, Elsevier Science Ltd., Amsterdam (1999) 156.
- [25] A.S. Hamada, M.C. Somani, L.P. Karjalainen: ISIJ Int. 47 (2007) 907. DOI:10.2355/isijinternational.47.907
- [26] M.C. Somani, D.A. Porter, A.S. Hamada, L.P. Karjalainen: Metall. Mater. Trans. A 46 (2015) 5329. DOI:10.1007/s11661-015-3112-0
- [27] A. Grajcar, R. Kuziak: Adv. Mater. Res. 287-290 (2011) 330. DOI:10.4028/www.scientific.net/AMR.287-290.330
- [28] A. Grajcar, R. Kuziak: Adv. Mater. Res. 314-316 (2011) 119. DOI:10.4028/www.scientific.net/AMR.314-316.119
- [29] N. Cabañas, N. Akdut, J. Penning, B.C. De Cooman: Metall. Mater. Trans. A 37 (2006) 3305. DOI:10.1007/BF02586165
- [30] S.F. Medina, J.E. Mancilla: ISIJ Int. 36 (1996) 1070. DOI:10.2355/isijinternational.36.1070
- [31] S.F. Medina, A. Quispe: ISIJ Int. 41 (2001) 774.
- DOI:10.2355/isijinternational.41.774
  [32] P.P. Suikkanen, V.T.E. Lang, M.C. Somani, D.A. Porter, L.P. Karjalainen: ISIJ Int. 52 (2012) 471. DOI:10.2355/isijinternational.52.471
- [33] L.P. Karjalainen: Mater. Sci. Technol. 11 (1995) 557. DOI:10.1179/mst.1995.11.6.557
- [34] L.P. Karjalainen, J. Perttula: ISIJ Int. 36 (1996) 729. DOI:10.2355/isijinternational.36.729
- [35] L.P. Karjalainen, J. Perttula, Y. Xu, J. Niu, in: Proc. 7th Int. Symp. Physical Simulation, Tsukuba, Japan (1997) 231.
- [36] S. Sakui, T. Sakai, K. Takeishi: Trans. Iron Steel Inst. Jpn. 17 (1977)718.
- [37] M.C. Somani, L.P. Karjalainen, J.H. Bianchi: Mater. Sci. Forum 558-559 (2007) 333. DOI:10.4028/www.scientific.net/MSF.558-559.333
- [38] L.P. Karjalainen, J.A. Koskiniemi, X.D. Liu, in: Proc. 37th Mechanical Working and Steel Processing Conf. & Int. Symp. Recovery and Recrystallization in Steel, Hamilton, Ontario, Vol. XXXIII (1995) 861.

- [39] P.D. Hodgson, R.K. Gibbs: ISIJ Int. 32 (1992) 1329. DOI:10.2355/isijinternational.32.1329
- [40] C.M. Sellars: Mater. Sci. Technol. 6 (1990) 1072. DOI:10.1179/mst.1990.6.11.1072
- [41] L.P. Karjalainen, in: Proc. 3<sup>rd</sup> Int. Conf. on HSLA Steels, The Chinese Society for Metals, Beijing (1995) 179.
- [42] V.T.E. Lang, P.P. Suikkanen, M.C. Somani, D.A. Porter, L.P. Karjalainen, in: Proc. Int. Sci. Technol. Conf. Advanced Metals, Materials and Technologies (AMMT'2011), St. Petersburg, Russia (2011) 301.
- [43] K. Airaksinen, L.P. Karjalainen, D. Porter, J. Perttula: Mater. Sci. Forum 284–286 (1998) 119. DOI:10.4028/www.scientific.net/MSF.284-286.119
- [44] L.P. Karjalainen, M.C. Somani, D.A. Porter: Mater. Sci. Forum 426–432 (2003) 1181. DOI:10.4028/www.scientific.net/MSF.426-432.1181

(Received July 3, 2018; accepted September 11, 2018; online since January 21, 2019)

### Correspondence address

Dr. Mahesh Chandra Somani University of Oulu Faculty of Technology Materials and Mechanical Engineering Post Box 4200 Oulu 90014 Finland Tel: +358294482144

Mobile: +358 294 482144 Mobile: +358 40 9662149 Fax: +358 8 344 084

e-mail: mahesh.somani@oulu.fi

Web: http://www.oulu.fi/materialsengineering/

### **Bibliography**

DOI 10.3139/146.111744 Int. J. Mater. Res. (formerly Z. Metallkd.) 110 (2019) 3; page 183–193 © Carl Hanser Verlag GmbH & Co. KG ISSN 1862-5282